Unit Cell Design for Intelligent Reflecting and Refracting Surface (IR^{2}S) with Independent Electronic Control Capability

Yujie Liu, *Member, IEEE*, James Kelly, *Member, IEEE*, Mark Holm, *Senior Member, IEEE,* Srikanth Gopal, Sina Rezaei Aghdam, *Member, IEEE* and Yuanwei Liu, *Senior Member, IEEE*

***Abstract*— This paper presents a design of an electronically reconfigurable Unit Cell (UC), that can be used in the construction of Intelligent Reflecting and Refracting Surfaces (IR^{2}Ss) for future 6G communication. It can independently perform beam forming or beam steering in both reflection and refraction modes. The IR^{2}S UC responds separately to TE and TM incidences. The UC utilizes PIN diodes to obtain two phase states, 0° and 180° (with 1-bit phase resolution), simultaneously in the reflection and refraction modes. Prototypes of the IR^{2}S UC have been fabricated and characterized in a waveguide measurement, showing excellent agreement between simulation and measurement at a centre frequency of 5.9 GHz.**

***Index Terms*— Reconfigurable intelligent surface, electronically beamforming, 1-bit transmit/reflect array, PIN diode.**

I. INTRODUCTION

INTELLIGENT reflecting and refracting surfaces (IR^{2}Ss) have emerged as a promising technology for enhancing the performance of wireless communication systems. They have been widely considered for use of sixth-generation (6G) communication networks as a way of controlling the path loss exponent, within an urban environment, and thus the S/I performance of mobile networks [1-3]. IR^{2}S can also enable real-time beamforming and beam steering, thereby helping to address areas subject to heavy multipath fading.

In the literature, there are numerous examples of UC designs used to construct the transmit/reflect arrays or metasurface that achieve bidirectional, multi-beam and beam steering capabilities [3-5]. For example, in [6], the author presents a UC consisting of just a single layer. The UC uses a PIN diode to alter the current distribution, resulting in phase modulation of the reflected signals. This enables the surface to scan in both azimuth and elevation planes at 5.8 GHz. Other 1-bit UC designs proposed in [7-9] have also been used for reflectarrays, achieving electronic beam scanning. However, these UC designs can only work in reflection mode, limiting their use to building the reflective surface. Similarly, in papers [10,11], 1-bit reconfigurable UCs have been proposed for transmitarrays, with the UCs being electronically controlled by diodes and

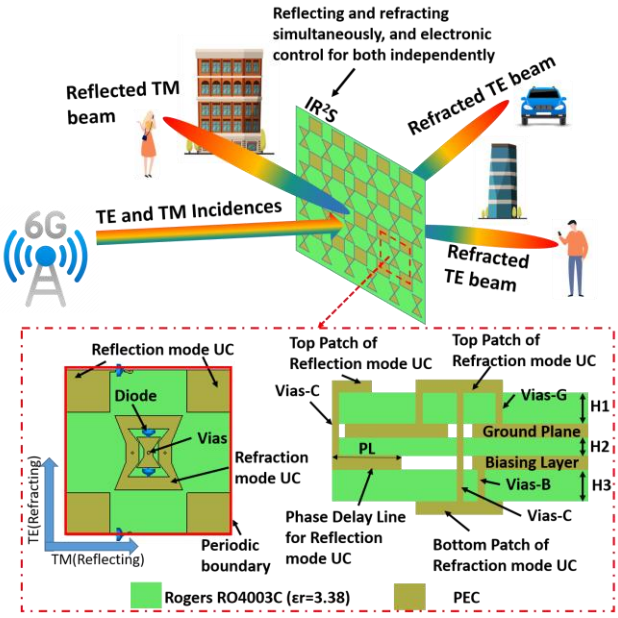

Fig. 1. The possible use case of the IR^{2}S in future networks, in which the IR^{2}S is based on the proposed UC design.

restricted to operating in only refraction mode. In [12-15], the authors provide insightful designs for UCs that exhibit the functionalities of reflecting and refracting simultaneously. The split-ring resonator [14] was used to constitute the UC structure, and the surface built with it can work in both reflection and refraction modes at 9.3 GHz with appropriate phase distribution. Unfortunately, these bidirectional beams are fixed and unable to steer. In [16], the author presents a single-layer sprit-ring UC with the ability to electronically scan both the reflected and refracted beams simultaneously. However, these two beams are not independently controllable. To our knowledge, designing the UCs for IR^{2}S application is still a challenging topic and one which has received relatively little attention in the literature [17]. The IR^{2}S implementation requires the UC structure that enables independent electronic

Yujie Liu, James Kelly, and Yuanwei Liu are with the School of Electronic Engineering and Computer Science, Queen Mary University of London, London E1 4NS, U.K. (e-mail: yujie.liu@qmul.ac.uk, j.kelly@qmul.ac.uk, yuanwei.liu@qmul.ac.uk).

Mark Holm, Srikanth Gopal and Sina Rezaei Aghdam are with the Radio Basestation Systems Department, Huawei Technologies (Sweden) AB, 412 50 Gothenburg, Sweden. (e-mail: mark.holm@huawei.com, srikanth.gopal@huawei.com, sina.rezaei.aghdam@huawei.com)

control of both reflected and refracted beams.

This paper proposes a design for a reconfigurable UC with independent electronic control, used for constructing the IR^{2}S. The proposed IR^{2}S UC comprises two modes of UCs: a sand-clock-slot UC for refraction mode and a rectangular-patch UC for reflection mode. They correspond to TE and TM mode incidences, respectively. Fig. 1 illustrates the possible use of the IR^{2}S constructed by our proposed UC, providing high adaptability to the 6G wireless communication system.

II. Unit Cell Design

Fig. 1 also shows the configuration of the IR^{2}S UC. It consists of three substrates and four metallic layers, and the substrates are all Rogers RO4003C with a permittivity of 3.38. A refraction mode UC is located at the centre and its four corners are formed from the four quarters of the reflection mode UC. To mimic an infinite array, periodic boundary conditions have been applied. The period of the IR^{2}S UC is 25 mm, which is the same as that of the individual reflection and refraction mode UCs.

In Fig. 2, the refraction mode UC consists of the bow-tie patches on the top and bottom layers, respectively. Both bow-tie patches incorporate the sand-clock-slots, while one side of the inner frame of the bottom patch is connected to the outer frame. The top patch incorporates two PIN diodes. The top and bottom patches are connected by metallized via-hole (Via-C) at the centre, and two vertical vias (Via-G) connect the ground plane and the outer frame of the top patch. The bottom patch connects to the biasing line through Via-B. Two PIN diodes on the top patch are orienting in opposite ways. Consequently, when one diode is biased in such a way as to turn it ON, the other is biased in such a way as to turn it OFF, and vice versa. A single pair of biasing lines are used to control both diodes. Thus, by changing the direction of the applied bias current from forward to reverse, the connection to the outer frame can be varied from the upper end to the lower end. When the TE wave propagates through this UC, the refraction is either in-phase or has a 180^o phase shift compared with the incident phase, depending on the direction of the biased current.

For the reflection mode UC, the patch is located on the top and connects to the ground plane through the Via-G. A PIN diode is placed at the side of the patch, linking it to the phase delay line, which is located on the biasing layer. Thus, the connection between the patch and the phase-delay line depends on the state of the PIN diode. By altering the states (i.e. ON or OFF) of the PIN diode, we can achieve the required phase difference of 180^o. An open-ended radial stub was used to choke the RF signal in the biasing line to ensure that the RF current did not flow on the DC line. Table I summarises the dimensions of the IR^{2}S UC. We set the width of the patches, 'RW' and 'Tw1', to approximate 10 mm, as this maintains a good performance and provides a good compromise between mutual coupling and the steering performance of the whole IR^{2}S. Considering the RF performances and cost, PIN diodes (BAR6402) are selected to control the UC performance electronically. The lumped element equivalent circuit for PIN

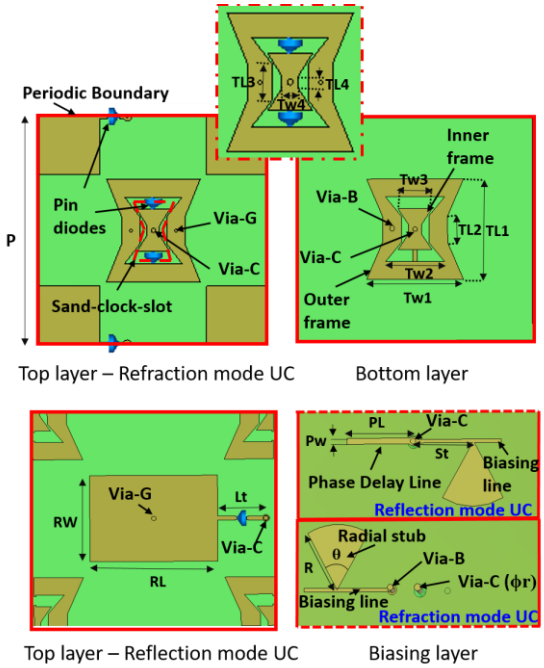

Fig. 2. Parameters details of each layer of the proposed IR^{2}S UC design.

TABLE I
DIMENSION OF THE PROPOSAL UNIT CELL (UNIT: MM)

Param.	P	RW	RL	Lt	Pw	PL	St
Value	25	10	13.3	5	0.5	8.6	7.7
Param.	TL1	TL2	TL3	TL4	Tw1	Tw2	Tw3
Value	11.3	3	3	1	10.3	6.3	3.6
Param.	R	θ	Tw4	ϕr	H1	H2	H3
Value	5	60^o	1.35	0.6	1.524	0.51	1.524

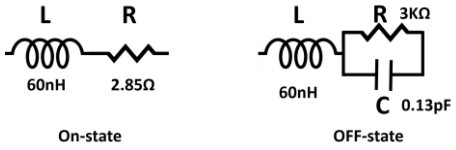

Fig. 3. The used equivalent circuit for the PIN diode (BAR6402).

diodes in the simulation is shown in Fig. 3. By biasing the diodes with forward and reverse currents, we can obtain different electromagnetic (EM) responses from the IR^{2}S UC. The IR^{2}S UC is capable of operating in refraction and reflection modes simultaneously, and these two modes can be controlled independently.

III. Fabrication and Measurement

The refraction mode UC and reflection mode UC do not have a common centre. Instead, there is spatial displacement between their centres. For this reason, it is impossible to create a single

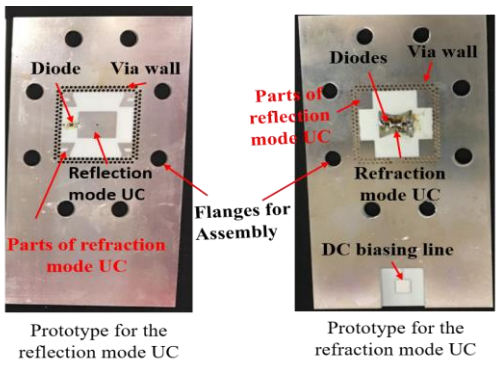

Fig. 4. The prototypes of IR^{2}S UC for refraction and reflection modes.

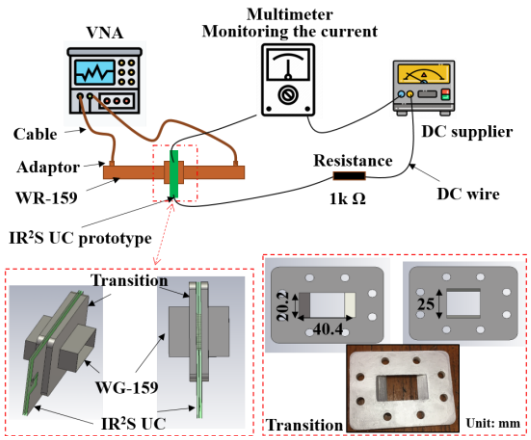

Fig. 5. The measurement setup for characterizing the IR^{2}S UC prototypes.

UC incorporating complete elements for both modes. An alternative approach would be to prepare a 2 by 2 arrangement of UCs. However, this would increase the size of the waveguide, leading to multi-mode propagation that would cause inaccuracies in the UC measurement. For these reasons, we then have prepared separate prototypes to characterise the performance, in each mode, through waveguide measurement. Fig. 4 shows the hardware prototypes for the IR^{2}S UC. The via wall is used to mimic the waveguide boundary condition and block the leakage of energy through the substrates. The forward or reverse bias can be applied through the extended DC biasing line, to switch the diodes between the ON and OFF states.

Fig. 5 shows the waveguide measurement setup that was used to characterise the IR^{2}S UC. A resistor with 1 KΩ was connected in series with PIN diodes to set and limit the current flowing into the diodes. The measurement setup is formed from two coax-to-WR159 adaptors, two WR159 straight sections of waveguide, and two tapered transitions between the rectangular section of the waveguide and the square section of the IR^{2}S UC. These transitions were used to convert the dimension of the waveguide to fit the UC size, effectively transitioning the dimension of 40.4 mm×21.2 mm (the waveguide) to 25 mm ×25 mm (the UC). The thickness of the transition was set to 4 mm (i.e. 0.08λ_o at 5.9 GHz) to ensure that the TE mode

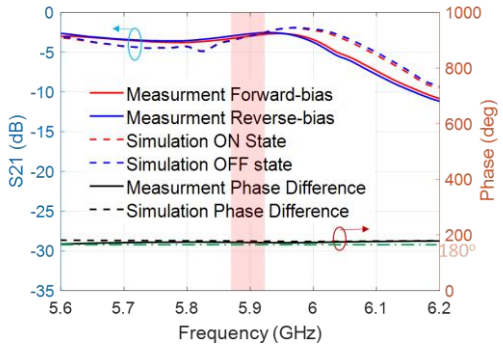

(a)

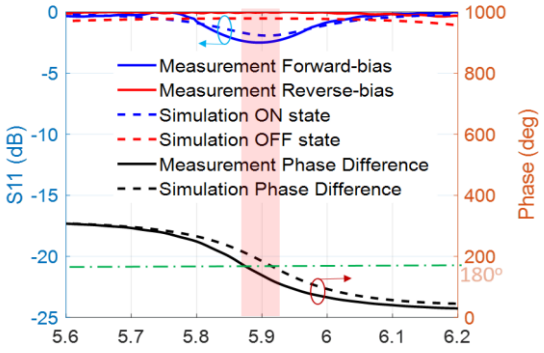

(b)

Fig. 6. The comparison results of measurement and simulation in (a) refraction and (b) reflection modes, under forward (ON state) and Reverse (OFF state) biasing of the pin-diode. Both working frequency bands range from 5.87-5.97 GHz, as shown by the pink bars.

propagation within the waveguide was not prevented by changes in cut-off frequencies (as a result of the dimension changes). Specifically, the result, in Fig. 6(a), shows that the refraction mode of IR^{2}S UC operates from 5.86 GHz to 5.97 GHz with an insertion loss of less than 3 dB. The phase difference between the ON and OFF states of diodes is maintained at 180^o across a wide frequency band. From the S11 plots in Fig. 6(b), we see what appears to be a resonance in the reflection mode of the IR^{2}S UC. This occurs when the diode is forward-biased, while no resonance occurs under reverse bias. This phenomenon results in a 180^o reflected phase difference at 5.9 GHz between the ON/OFF states of the diode, allowing the IR^{2}S UC to operate from 5.87 GHz to 5.95 GHz with the reflected phase difference varying between 160^o and 200^o.

IV. Results and Discussion

Based on the UC performance, we have constructed an array comprising 13×13 elements. This array incorporates a dual-polarized patch antenna that is employed as a feeding antenna. The feeding antenna provides TE and TM incident waves. In order to ensure efficient coupling of energy into the surface, we have calculated the optimum -10 dB beamwidth for the surface. In turn, this can be used to calculate the F/D (Focus to Dimension) ratio of the IR^{2}S, yielding a value of 0.42.

TABLE II
PERFORMANCE COMPARISON WITH PREVIOUS RESEARCH

Reference	Working frequency	Beam types	No. substrates	Reflecting or Refracting	Scanned range of the surface	Independent control
[6]	5.8 GHz	Beam Steering	1	Only reflecting	[0°,60°]	Yes
[11]	26 GHz	Beam Steering	2	Only refracting	Not provided	Yes
[13]	9.3 GHz	Fixed Beam	2	Simultaneously	Unable to steer	No
[15]	10 GHz	Fixed Beam	3	Either reflecting or refracting	Unable to steer	No
[16]	5.35 GHz	Beam Steering	1	Simultaneously	[0°,60°]	No
[17]	9.5 GHz	Beam Steering	4	Simultaneously	[0°,40°]	Yes
This work	5.9 GHz	Beam Steering	3	Simultaneously	[0°,60°]	Yes

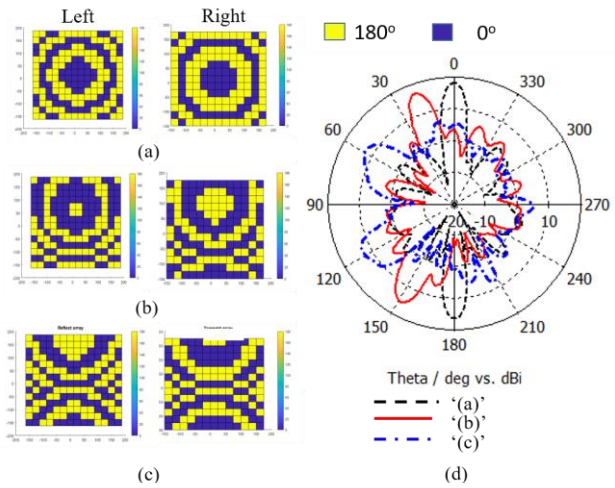

Fig. 7. Phase distributions for both reflection (left: θ_R, φ_R) and refraction modes (right: θ_T, φ_T) under various conditions: (a) (θ_R=0°, φ_R =0°) and (θ_T=0°, φ_T =0°), (b) (θ_R=20°, φ_T =0°) and (θ_T=150°, φ_T =0°), (c) (θ_R=60°, φ_R =0°) and (θ_T=120°, φ_T =0°), respectively. (Here, 'θ' represents the elevation angle, and 'φ' represents the azimuth angle.) (d) Radiation performance at 5.9 GHz under these conditions.

It is also necessary to properly configure the phase distribution across the surface to enable dynamic beam steering. This can be calculated using (1) and discretized into two phase states namely 0° and 180°. In practice, this discretization process can be achieved by forward or reverse biasing the pin diodes in each individual element of the UC. Fig. 7 shows the calculated phase distributions for beams in the reflection and refraction modes, covering various scenarios. In each example the main beam points towards a different direction. Fig. 7 also shows the radiation performance corresponding to various examples of phase distribution. Notably, in both the reflection and refraction modes, we demonstrate the capability to achieve beam scanning from 0° to 60°.

$$\Psi(x_i, y_j) = k_0[d_{i,j} - (x_i cos\varphi_0 + y_j sink\varphi_0) \times sin\theta_0]$$

$$= \begin{cases} 0^0, mod(\Psi(x_i, y_i), 360) \in [0^0, 180^0) \\ 180^0, mod(\Psi(x_i, y_i), 360) \in [180^0, 360^0) \end{cases} \quad (1)$$

where $\Psi(x_i, y_j)$ is the compensation phase for the element at position (x_i, y_j). k_0 is the free space wavenumber and $d_{i,j}$ is the distance between the feeding focus point to the $(i,j)^{th}$ element. (θ_0, φ_0) represents the beam targeting direction.

Table II provides a comparison between our proposed IR²S UC and other reported UC designs. It also includes the surface performance constructed by these UCs. The focus of the comparison is on whether the UC designs enable simultaneous beam steering in refraction and reflection modes and independent electronic control of them, and the scanned range of their surfaces. The bandwidth performance is not considered. The UC designs proposed in [6] and [11], enable electronic beam steering using one or two substrates, but only for the reflection mode. The UC structures presented in [13] and [16] enable the refraction and reflection modes to be obtained simultaneously. However, they can only generate fixed beams and do not allow for individual control of beams produced in the refraction and reflection modes. The surface design reported in [17] meets the requirements for IR²S applications, enabling independent control of refracted and reflected beams, but its scanned range is restricted to 0° to 40°. In comparison to recent UC designs, our proposed IR²S UC has the advantage of simultaneous beam steering in both refraction and reflection modes, with independent electronic control. Its surface also demonstrates the advantage of requiring fewer substrates, and yet provides broader scanning capabilities, from 0° to 60°, in both reflection and refraction modes, compared to [17]. These reveal the practicality of the proposed UC and its applicability for use within an IR²S surface.

V. CONCLUSION

In conclusion, this paper presents a reconfigurable UC that realizes independent electronic control for both refraction and reflection modes. The UC's performance has demonstrated its suitability for constructing the IR²S. Dynamic beams have also been verified with providing a scanned range from 0° to 60°, in both modes. The UC offers a promising solution for future 6G communication.

ACKNOWLEDGEMENT

This work was supported by Huawei Technologies Sweden AB.

REFERENCES

[1] Y. Liu et al., "Reconfigurable Intelligent Surfaces: Principles and Opportunities," in IEEE Communications Surveys & Tutorials, vol. 23, no. 3, pp. 1546-1577, third quarter 2021.
[2] H. Zhang et al., "Intelligent Omni-Surfaces for Full-Dimensional Wireless Communications: Principles, Technology, and Implementation," in IEEE Communications Magazine, vol. 60, no. 2, pp. 39-45, February 2022.
[3] Li, W., Ma, Q., Liu, C. et al. Intelligent metasurface system for automatic tracking of moving targets and wireless communications based on computer vision. Nat Commun 14, 989 (2023).
[4] S. Zeng et al., "Intelligent Omni-Surfaces: Reflection-Refraction Circuit Model, Full-Dimensional Beamforming, and System Implementation," in IEEE Transactions on Communications, vol. 70, no. 11, pp. 7711-7727, Nov. 2022.
[5] Cui, T., Qi, M., Wan, X. et al. Coding metamaterials, digital metamaterials and programmable metamaterials. Light Sci Appl 3, e218 (2014).
[6] G. C. Trichopoulos et al., "Design and Evaluation of Reconfigurable Intelligent Surfaces in Real-World Environment," in IEEE Open Journal of the Communications Society, vol. 3, pp. 462-474, 2022.
[7] F. Wu, R. Lu, J. Wang, Z. H. Jiang, W. Hong and K. -M. Luk, "A Circularly Polarized 1 Bit Electronically Reconfigurable Reflectarray Based on Electromagnetic Element Rotation," in IEEE Transactions on Antennas and Propagation, vol. 69, no. 9, pp. 5585-5595, Sept. 2021.
[8] Z. Wang et al., "1 Bit Electronically Reconfigurable Folded Reflectarray Antenna Based on p-i-n Diodes for Wide-Angle Beam-Scanning Applications," in IEEE Transactions on Antennas and Propagation, vol. 68, no. 9, pp. 6806-6810, Sept. 2020.
[9] S. Tian, H. Liu, and L. Li, “Design of 1-Bit Digital Reconfigurable Reflective Metasurface for Beam-Scanning,” Applied Sciences, vol. 7, no. 9, p. 882, Aug. 2017.
[10] L. Di Palma, A. Clemente, L. Dussopt, R. Sauleau, P. Potier and P. Pouliguen, "1-Bit Reconfigurable Unit Cell for Ka-Band Transmitarrays," in IEEE Antennas and Wireless Propagation Letters, vol. 15, pp. 560-563, 2016.
[11] M. T. Nguyen and B. D. Nguyen, "1-bit Unit-Cell For Ka-band Reconfigurable Transmitarrays," 2021 International Symposium on Antennas and Propagation (ISAP), Taipei, Taiwan, 2021, pp. 1-2.
[12] W.Yang, K. Chen, and Y. Feng. "Multifunctional Metasurface for Broadband Reflect-Transmit-Array Antenna at 5G Millimeter-Wave Band." 2022 16th European Conference on Antennas and Propagation (EuCAP). IEEE, 2022.
[13] H. -X. Xu et al., "Multifunctional Microstrip Array Combining a Linear Polarizer and Focusing Metasurface," in IEEE Transactions on Antennas and Propagation, vol. 64, no. 8, pp. 3676-3682, Aug. 2016.
[14] L. -X. Wu, K. Chen, T. Jiang, J. Zhao and Y. Feng, "Circular-Polarization-Selective Metasurface and Its Applications to Transmit-Reflect-Array Antenna and Bidirectional Antenna," in IEEE Transactions on Antennas and Propagation, vol. 70, no. 11, pp. 10207-10217, Nov. 2022.
[15] M. Wang, S. Xu, F. Yang and M. Li, "A 1-Bit Bidirectional Reconfigurable Transmit-Reflect-Array Using a Single-Layer Slot Element With PIN Diodes," in IEEE Transactions on Antennas and Propagation, vol. 67, no. 9, pp. 6205-6210, Sept. 2019.
[16] Y. Li, Y. Wang and Q. Cao, "Design of a Multifunctional Reconfigurable Metasurface for Polarization and Propagation Manipulation," in IEEE Access, vol. 7, pp. 129183-129191, 2019.
[17] H. Yu, P. Li, J. Su, Z. Li, S. Xu and F. Yang, "Reconfigurable Bidirectional Beam-Steering Aperture With Transmitarray, Reflectarray, and Transmit-Reflect-Array Modes Switching," in IEEE Transactions on Antennas and Propagation, vol. 71, no. 1, pp. 581-595, Jan. 2023.